

Global warming is projected to lead to increased freshwater growth potential and changes in pace of life in Atlantic salmon *Salmo salar*

Adrian Rinaldo^{1,2,3}  | Elvira de Eyto² | Thomas Reed^{1,3} | Karl Øystein Gjelland⁴ | Philip McGinnity^{1,3}

¹School of Biological, Earth and Environmental Sciences, University College Cork, Cork, Ireland

²Fisheries Ecosystems Advisory Services, Marine Institute, Newport, Ireland

³Environmental Research Institute, University College Cork, Cork, Ireland

⁴Norwegian Institute for Nature Research, Tromsø, Norway

Correspondence

Adrian Rinaldo, School of Biological, Earth and Environmental Sciences, University College Cork, Distillery Fields, North Mall Campus, University College Cork, T23 N73K Cork, Ireland.

Email: ARinaldo@ucc.ie

Funding information

HORIZON EUROPE Marie Skłodowska-Curie Actions, Grant/Award Number: 956623; Marine Institute Grant-in-Aid, Grant/Award Number: RESPI/BIO/21/01; Science Foundation Ireland, Grant/Award Numbers: 15/IA/3028, 16/BBSRC/3316

Abstract

Global warming has been implicated in widespread demographic changes in Atlantic salmon *Salmo salar* populations, but projections of life-history responses to future climate change are lacking. Here, we first exploit multiple decades of climate and biological data from the Burrishoole catchment in the west of Ireland to model statistical relationships between atmospheric variables, water temperature, and freshwater growth of juvenile Atlantic salmon. We then use this information to project potential changes in juvenile growth and life-history scheduling under three shared socioeconomic pathway and representative concentration pathway scenarios from 1961 to 2100, based on an ensemble of five climate models. Historical water temperatures were well predicted with a recurrent neural network, using observation-based atmospheric forcing data. Length-at-age was in turn also well predicted by cumulative growing degree days calculated from these water temperatures. Most juveniles in the Burrishoole population migrated to sea as 2-year-old smolts, but our future projections indicate that the system should start producing a greater proportion of 1-year-old smolts, as increasingly more juveniles cross a size-based threshold in their first summer for smoltification the following spring. Those failing to cross the size-based threshold will instead become 2-year-old smolts, but at a larger length relative to 2-year-old smolts observed currently, owing to greater overall freshwater growth opportunity. These changes in age- and size-at-seaward migration could have cascading effects on age- and size-at-maturity and reproductive output. Consequently, the seemingly small changes that our results demonstrate have the potential to cause significant shifts in population dynamics over the full life cycle. This workflow is highly applicable across the range of the Atlantic salmon, as well as to other anadromous species, as it uses openly accessible climate data and a length-at-age model with minimal input requirements, fostering improved general understanding of phenotypic and demographic responses to climate change and management implications.

KEYWORDS

aquatic ectotherms, growing degree days, ISIMIP, life history, population dynamics

This is an open access article under the terms of the [Creative Commons Attribution](https://creativecommons.org/licenses/by/4.0/) License, which permits use, distribution and reproduction in any medium, provided the original work is properly cited.

© 2023 The Authors. *Journal of Fish Biology* published by John Wiley & Sons Ltd on behalf of Fisheries Society of the British Isles.

1 | INTRODUCTION

The Earth's climate is warming (IPCC, 2022), leading to changes in near-surface air temperature, humidity, air pressure, wind, and precipitation, which in turn influences ecosystems across multiple levels (i.e., individual, population, and community) (Woodward et al., 2010). Species may respond to changes in their environment by phenotypic plasticity, evolutionary adaptation, or migration (Sears & Angilletta, 2011). However, changes are happening at an unprecedented rate, and many species may be unable to adapt quickly enough to avoid population decline and possible extinction (Radchuk et al., 2019; Reed, Schindler, & Waples, 2011). This is particularly the case for species that undertake seasonal migrations, as successful migration relies on fine-tuned responses to environmental cues (Crozier et al., 2008). The adaptation of migratory individuals to their surroundings manifests in their life-history traits such as growth pattern, age- and size-at-migration, and reproduction timing. Juvenile Atlantic salmon *Salmo salar* L. 1758 typically spend 1–5 years in fresh water before undergoing the physiological smoltification process and migrating to sea as smolts. They then spend between one and three winters at sea, before completing the life cycle by returning to spawn. A decrease in the age-at-smoltification with increasing temperatures has already been observed in some populations (Russell et al., 2012; Thorstad et al., 2021). Widespread recent declines in Atlantic salmon stocks appear to be driven predominantly by declines in marine survival, possibly related to climate change (ICES, 2022). Climate-driven impacts in fresh water can also directly affect population dynamics via reductions in smolt numbers, or indirectly via carry-over effects on marine survival and growth, and the number of years spent at sea (Mobley et al., 2021). It is, therefore, crucial to quantify and understand how juvenile Atlantic salmon will respond to climate change across their native range in the coming decades.

The Atlantic salmon is native to river systems draining into the North Atlantic Ocean, the Baltic Sea, and the Barents Sea (Klemetsen et al., 2003; MacCrimmon & Gots, 1979; Thorstad et al., 2011, 2021). Atlantic salmon that occur in linked river and ocean systems are within their physiological requirements for temperature (see Bennett et al., 2021). Lower and upper thermal limits are 0 and 27°C, respectively, for juvenile life stages (Elliott, 1991; Elliott & Elliott, 2010; Jensen et al., 1991; Thorstad et al., 2021), with growth occurring between 7 and 23°C with an optimum of 15.9°C (Elliott & Hurley, 1997). The effects of climate change are expected to be most prominent for the populations at or close to the edges of the distribution range (Thorstad et al., 2021), with the southernmost populations disappearing, and the northernmost populations experiencing significant changes in life-history and, consequently, population dynamics.

Physiological processes in ectotherms are dependent on ambient temperatures (Atkinson, 1994; Hazel & Prosser, 1974; Van Der Have & De Jong, 1996), but the precise relationship between temperature and growth in ectotherms is uncertain (Sears & Angilletta, 2011). Cumulative growing degree days (CGDD) is the accumulation of ambient temperatures over time relevant for growth and development in

ectotherms, and this metric of physiological time is widely applied in agronomy and entomology (Neuheimer & Taggart, 2007). The use of CGDD in fish ecology is increasing, and several studies show strong linear correlations between CGDD and growth in immature fish (Chezik et al., 2014; Neuheimer & Taggart, 2007; Venturelli et al., 2010). Growth in juvenile Atlantic salmon is controlled by both intrinsic and extrinsic factors. Temperature and photoperiod are key determinants of both internal (e.g., physiological processes) and external (e.g., resource availability) processes, varying substantially across seasons. Because CGDD integrates time and temperature, the method offers good possibilities for investigating the effects of climate change on growth, and subsequent changes in life history of juvenile Atlantic salmon.

Recent reviews of climate change effects on Atlantic salmon suggest that changes in water temperature and hydrology will cause significant shifts in life-history traits such as growth and age- and size-at-smoltification with cascading effects on age- and size-at-maturity, pace of life and ultimately reproductive output (Jonsson & Jonsson, 2009; Thorstad et al., 2021). Consequently, seemingly small changes in the life history of juvenile Atlantic salmon may cause significant changes in population dynamics. Moving from qualitative explorations to quantitative projections can be supported by the development and validation of models that can then be driven by future climate projections.

Quantitative approaches have been developed to investigate climate change impacts on Atlantic salmon. For example, Hedger et al. (2013), Piou and Prévost (2012) and Sundt-Hansen et al. (2018) have used individual-based models to quantify individual and population-level responses to changes in climate. However, these studies build on large amounts of observational data (e.g., discharges, fish density estimates, genetics), to calibrate and parameterize the models to specific populations. The data requirements of these approaches make them difficult to apply to broad spatial scales such that they are applicable to populations across the distribution range of the species. We sought to design a model workflow quantifying the impact of global warming on a key life-history trait in the Atlantic salmon, which would be applicable across the distribution range for both data-poor and data-rich populations. The Intersectoral Impact Model Intercomparison Project (ISIMIP) offers a framework for consistently projecting the impacts of climate change across affected sectors and spatial scales (Frieler et al., 2017), which is well suited to the Atlantic salmon as it inhabits a wide geographic area and several distinct habitats (e.g., freshwater, coastal, and marine).

The overarching aim of this study is to develop a modeling workflow that ties atmospheric climate data to the key life-history traits size- and age-at-smoltification via freshwater growth. Specifically, we (1) statistically model a relationship between atmospheric data ISIMIP phase 3a and in-situ water temperature using a neural network approach; (2) establish a statistical relationship between length-at-age and CGDD using a generalized linear model; (3) couple the water temperature model with the length-at-age model, and future climate projections from ISIMIP phase 3b; and (4) analyse the life-history response using a calibrated reaction norm for smoltification.

2 | MATERIALS AND METHODS

2.1 | Study site

The Burrishoole catchment (53°56' N, 9°35' W) is situated in the west of Ireland. The catchment is ~100 km² in size and consists of lakes and streams draining into the northeast Atlantic Ocean through Clew Bay (Figure 1). Due to the temperate oceanic climate, air temperatures historically rarely exceed 20°C, and the minimum water temperature is typically between 2 and 4°C (de Eyto et al., 2022).

Monitoring of diadromous fish in the Burrishoole catchment began in the late 1950s. Complete monitoring of migrating diadromous fish has been in place since 1970, with sea-entry traps on the Mill Race and Salmon Leap (Figure 1). Atlantic salmon in the Burrishoole catchment migrate as 1- to 3-year-old smolts from March to June, with more than 90% migrating as 2-year-olds (Piggins & Mills, 1985). The annual number of smolts declined from ~16,000 in the 1970s to around 5500 in the mid-to-late 2010s (Marine Institute, 2020).

2.2 | Model workflow

To investigate the effects of climate change on juvenile Atlantic salmon in the Burrishoole, a multistep workflow was developed using

Python (Van Rossum & Drake, 2010). The multistep workflow consists of four main steps: (1) statistical modeling of water temperatures from atmospheric data; (2) statistical modeling of length-at-age from CGDD calculated from modeled water temperature; (3) coupling of the water temperature model, the length-at-age model, and future climate projections; and (4) analysis of life-history response (Figure 2). Multiple substeps to the workflow are only briefly described, but more detailed descriptions are found in the supplementary material S1a, S1b, S2, S3, S4 and S5.

This study uses climate data from the ISIMIP as it provides a framework to assess the effects of climate change by offering openly accessible historical and current data, and future climate projections (Frieler et al., 2017). The ISIMIP consists of several phases: phase 3a provides climate reanalysis data from the historical to contemporary climate, and phase 3b provides historical, current, and three future climate scenarios based on the combination of three shared socioeconomic pathways and representative concentration pathways (i.e., SSP-RCPs) (<https://www.isimip.org/>). In short, the three SSP-RCP scenarios denote the socioeconomic trends in combination with the level of greenhouse gas (GHG) emissions, with SSP1-RCP2.6 being a low emission scenario, SSP3-RCP7.0 a medium to high emission scenario, and SSP5-RCP8.5 a high emission scenario (see Meinshausen et al., 2011; Riahi et al., 2017). The ISIMIP phase 3a and 3b data applied in this study have a daily temporal and 0.5° latitude × longitude spatial resolution and comprise near-surface air temperature (°C), near-surface wind speed (m s⁻¹), precipitation (kg m⁻² s⁻¹), snowfall flux (kg m⁻² s⁻¹), surface downwelling shortwave radiation (W m⁻²), surface downwelling longwave radiation (W m⁻²), near-surface specific humidity (unitless), and near-surface relative humidity (%).

2.2.1 | Step 1: Water temperature model

To establish a link between atmospheric conditions and water temperatures, daily average in-situ water temperatures (1961–2019) from the Burrishoole catchment were obtained from the Marine Institute Ireland (Marine Institute Ireland, doi: 10/cvft), measured in the Mill Race (Figure 1). Historical to concurrent climate reanalysis data (i.e., GSWP3-W5E5 observation-based, climate-related forcing data) were obtained from ISIMIP phase 3a (1961–2019). To retain as much data as possible, missing values in the Mill Race time series were linearly interpolated if the consecutive number of missing values was less than 30 days. If the number of consecutive missing values was more than 30 days, the entire year was removed from the time series. The years 1965, 1967, 1974, 1991, 2012, 2013, and 2017 were excluded due to extended periods of missing data, and 1990 and 2005 were removed due to calibration and sensor issues (E. de Eyto, pers. comm.).

The in-situ water temperature and modeled atmospheric data were merged, centered, and scaled according to quantile range scaling using RobustScaler from the scikit-learn module (Pedregosa et al., 2011). Information on seasonality was encoded using sine and cosine transformations of the day of year, which results in equal

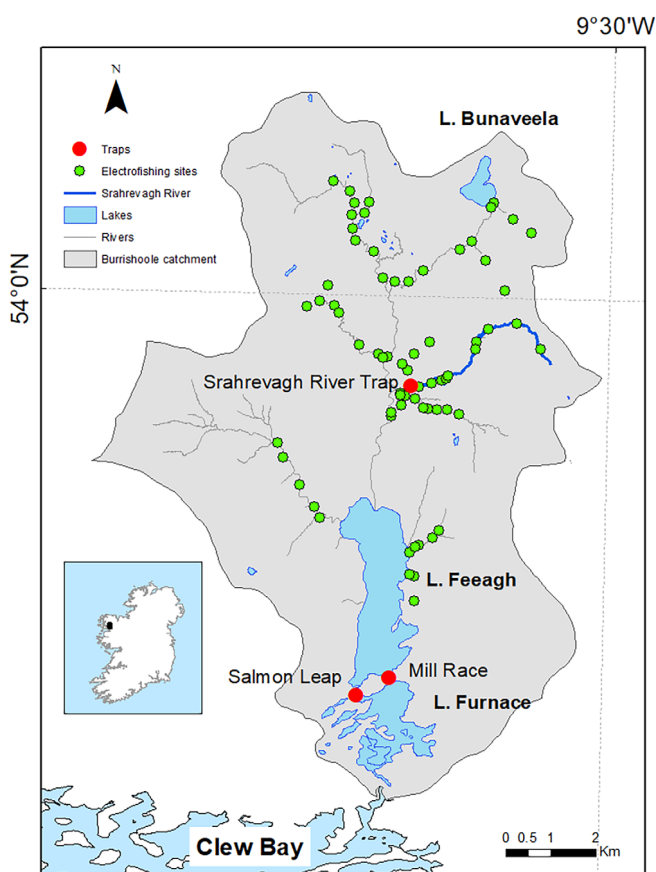


FIGURE 1 Location of electrofishing sites (green circles) and fish traps (red circles) in the Burrishoole catchment, Co. Mayo, Ireland.

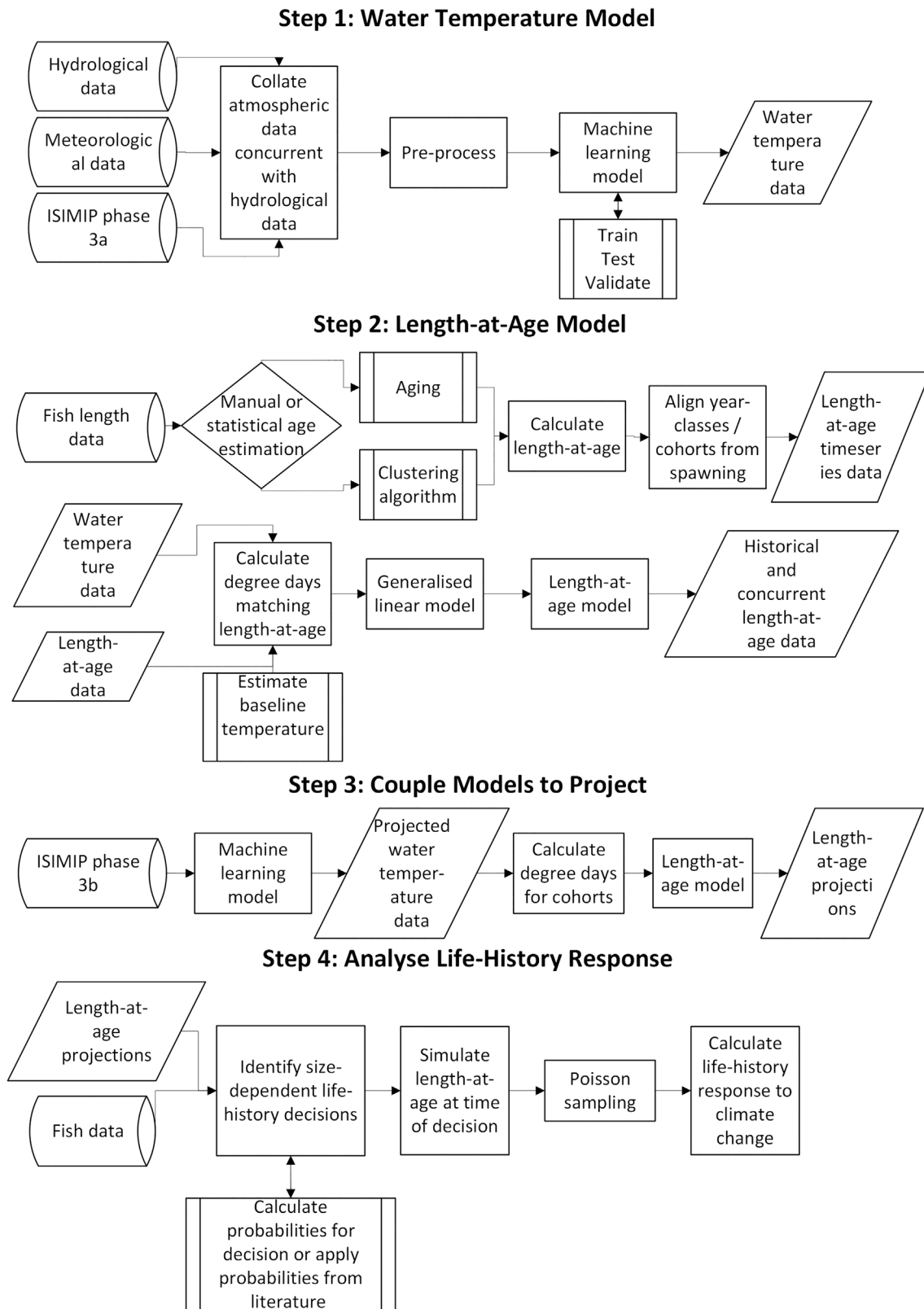


FIGURE 2 The four-step model workflow for quantitatively estimating length-at-age and life history of juvenile Atlantic salmon in response to climate change. Step 1 describes the collation of necessary data and construction of the water temperature model. Step 2 details the data preparation and construction of the length-at-age model for juvenile Atlantic salmon. Step 3 shows the coupling of the ISIMIP phase 3B projections to the water temperature model, and the subsequent coupling with the length-at-age model. Step 4 shows the post-processing of length-at-age projections to estimate smoltification probability and proportion of 1-, 2- and 3-year-old smolts. Shapes are according to ISO 5807 standard.

spacing between every date (e.g., day 365 is as close to day 1 as day 1 is to day 2). The merged dataset was then split into a training (1961–1994) subset and a validation (1995–2019) subset. A long short-term memory neural network (i.e., LSTM) was selected based on fidelity of multiple approaches measured by mean absolute error (i.e., MAE) and mean root squared error (i.e., RMSE) (see supplementary material S1a).

The LSTM neural network allows for modeling of nonlinear relationships and was constructed of a masking layer, an LSTM layer with 16 nodes and a tanh activation function, a dropout layer with a dropout rate of 0.2 to prevent overfitting, and a dense layer with a single node using a linear activation function. Additionally, a call-back function based on the validation RMSE and patience of 10 epochs was specified to prevent overfitting (see supplementary material S1b). The LSTM neural network was set up using the TensorFlow and Keras modules (Abadi et al., 2016; Chollet, 2013).

2.2.2 | Step 2: Length-at-age model

To assess the effect of water temperature on juvenile Atlantic salmon, fish length data from three sources within the Burrishoole catchment were obtained (Figure 1). First, annual catchment-wide electrofishing surveys are carried out every year between July and October at approximately 40 sites distributed across the catchment. Body lengths of 30,912 wild juvenile Atlantic salmon belonging to 20 cohorts from these surveys were extracted from 2000 to 2019. Second, high-resolution monitoring is carried out in the Srahrevagh River using a fish trap to capture all life-history stages from swim-up fry to sea-migrating smolts (McGinnity et al., 1997). These records include measured body lengths of 2999 wild juvenile Atlantic salmon belonging to nine cohorts sampled between 1998 and 2017. Finally, a subsample of migrating smolts that is killed for biometric sampling each year at the Mill Race and Salmon Leap Traps, and body lengths from 3366 Atlantic salmon smolts belonging to 20 cohorts sampled between 2000 and 2019 were included. In total, information on 37,277 individual fish was collated, but after the removal of outliers and observations with missing values, the number of fish in the analysis was reduced to 37,258 juvenile Atlantic salmon. A further reduction to the sample number was undertaken due to missing water temperature data for years after 2019, and so the final number of fish in the analysis was brought down to 35,719. In all cases, body length is expressed as the fork length.

After amalgamation of fish body length data, age classification was performed based on body length and time of capture using a Gaussian mixture model (with the expectation-maximization algorithm) from the scikit-learn module (Pedregosa et al., 2011). A sliding window technique was used to subdivide the year into shorter time periods accounting for growth. Backcalculation of age in days for each fish was done using a 2-year smolt trajectory and a fixed date for egg deposition in the riverbed substrate, allowing for alignment of cohorts consistent with Gregorian calendar years. The fixed egg deposition was set as the date of winter solstice (i.e., 21st of December), which

falls well within the spawning window of adult Atlantic salmon in the Burrishoole (see supplementary material S2).

The CGDD for each cohort was calculated from the date of fixed egg deposition and for the entire freshwater residency using Equation (1),

$$CGDD = \sum_{i=1}^n T_d - T_b, \quad (1)$$

where T_d is the daily mean water temperature obtained from the LSTM neural network predictions using climate reanalysis data, and T_b is the lower threshold temperature for growth (i.e., baseline temperature). Based on repeated iterations of an ordinary least squares (OLS) model with varying baseline temperatures, T_b was set to 0°C based on the highest coefficient of determination and lowest AIC (see supplementary material S3).

Multiple length-at-age models were then parameterized linking body length (mm) to CGDD (°C · day) using the Statsmodels module (Seabold & Perktold, 2010). Based on model fidelity, a generalized linear model using the gamma distribution and natural logarithmic link function was selected (see supplementary material S4). The 95% prediction interval for the model was obtained by normal approximation of the sampling distribution of the coefficients with 50,000 random draws.

2.2.3 | Step 3: Coupling of models and projection

To generate future projections of water temperatures for the Mill Race, atmospheric data produced by five general circulation models (i.e., GFDL-ESM4, IPSL-CM6A-LR, MPI-ESM1-2-HR, MRI-ESM2-0, and UKESM1-0-LL) for the SSP-RCP 1–2.6, 3–7.0, and 5–8.5 climate scenarios (2020–2100) were obtained from ISIMIP phase 3b for the 0.5° latitude × longitude grid cell overlying the Burrishoole catchment.

These data were used to simulate future water temperatures by forcing the LSTM neural network derived in Step 1, and the ensemble mean was calculated and used to determine the number of CGDD experienced and body length achieved for every cohort from 2021 to 2098 using the length-at-age model derived in Step 2.

2.2.4 | Step 4: Analysis of life-history response

To investigate the response of juvenile Atlantic salmon to climate change, the body length distribution was simulated for a total of 10,000 fish per cohort using a normal approximation of the sample distribution of the coefficient (i.e., the prediction interval) at three key time points via the length CGDD model: (1) first decision window for smoltification; (2) time of seaward migration for 1-year-old smolts; and (3) time of seaward migration for 2-year-old smolts. We further assume no early maturation of male parr due to no available records. The probability for smoltification as a 1-year-old was calculated using Equation (2):

$$\begin{aligned}
 P(\text{will smolt next spring}) & \\
 &= 1 - P(\text{will not smolt next spring}) \quad (2) \\
 &= 1 - (e^{52.321 - 0.862 \cdot \text{FL}}),
 \end{aligned}$$

where FL is body length expressed as fork length (adapted from Metcalfe, 1998 [p. 99, Table 1]), and iteratively calibrated to the smolt run of 1983 reported in Piggins and Mills (1985). Using Poisson sampling (i.e., independent Bernoulli trials) and a uniform probability distribution, each fish was assigned to one of two alternative categories: “will smolt as a 1-year-old” (success) or “will not smolt as a 1-year-old” (failure). Subsequently, for fish in the “will not smolt as a 1-year-old” category the probability of being a smolt as a 2-year-old was calculated using Equation (3):

$$P(\text{immature fish is now smolt}) = e^{0.0823 \cdot \text{FL} - 8.774}, \quad (3)$$

where FL is body length expressed as fork length and iteratively calibrated to the smolt run of 1983 reported in Piggins and Mills (1985). Again, using

TABLE 1 Ordinary least squares regression of annual average water temperature as a function of year for observed and modeled water temperature in the Mill Race (Burrishoole Catchment, Co. Mayo, Ireland).

| | Observed average water temperature (°C year ⁻¹) | Modeled average water temperature (°C year ⁻¹) |
|---------------------|---|--|
| Intercept | -35.250*** (8.633) | -23.940*** (6.316) |
| Year | 0.023 *** (0.004) | 0.017*** (0.003) |
| R ² | 0.368 | 0.344 |
| R ² adj. | 0.355 | 0.333 |
| N (DF) | 50 (48) | 58 (56) |

Note: Water temperature was modeled using a long short-term memory neural network. Standard error in parentheses. * $p < 0.1$; ** $p < 0.05$; *** $p < 0.01$.

Abbreviation: DF, degrees of freedom.

Poisson sampling and a uniform probability distribution, non-smolts were assigned to the either of two categories: “are now 2-year-old smolts” (success) or “will not smolt as a 2-year-old” (failure). The remaining fish that did not smolt as 1- or 2-year-olds were then considered to be 3-year-old smolts (more detail is contained in supplementary material S5).

The impact of climate change on smolt age composition was then calculated for each cohort, and the underlying trend was quantified using OLS regression. Lastly, the length distribution of 1-year- and 2-year-old smolts was visualized over time using the JoyPy module.

2.3 | Ethics statement

Ethical review and approval was not required for this study because the data used in this article were collected by the Irish Marine Institute for stock assessment purposes and therefore does not fall under the EU and Irish directives on animal welfare (2010/63/EU, SI No 543 of 2012). The sampling infrastructure (fish traps) operates under license (Fisheries Acts 1959–2003) from the Department of Agriculture, Food and Marine and by permission of the Minister of Agriculture, Food and Marine.

3 | RESULTS

3.1 | Historic to contemporary

3.1.1 | LSTM neural network

Comparison of in-situ and statistically modeled water temperature in the Mill Race showed close agreement for the training period (1961–1994) with an RMSE = 0.654°C and MAE = 0.488°C, and the validation period (1995–2019) with an RMSE = 0.844°C and MAE = 0.633°C (Figure 3). Due to the model setup, the year 1961 is

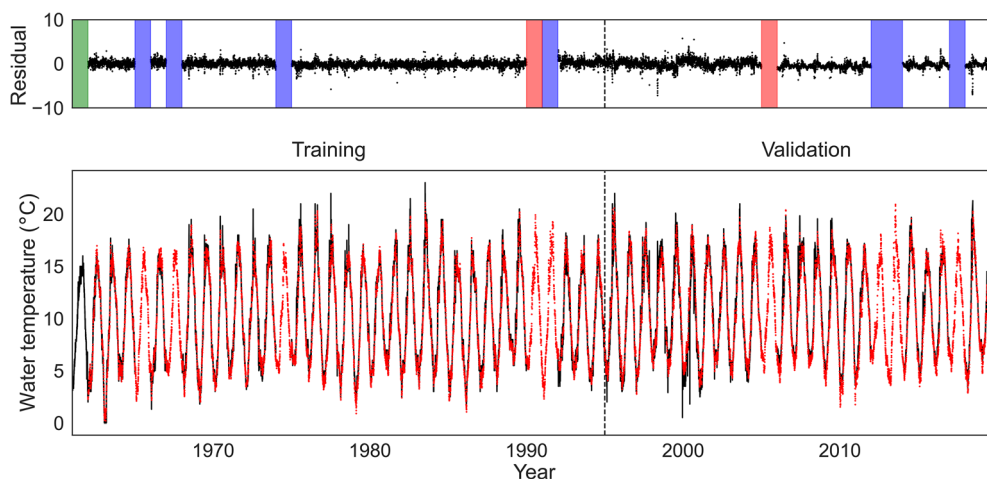


FIGURE 3 The residual error between observed and predicted water temperature (top panel), and the in-situ water temperature (black line) and long short-term memory neural network water temperature prediction (red crosses) for the training (1961–1994) and validation (1995–2019) dataset in the Mill Race (bottom panel). Years excluded due to accumulation of internal sate (green), prolonged periods of missing data (blue shaded), and measurement error (red shaded) are shown in the top panel, and the delineation of the training and validation period is shown by the vertical dashed line in both panels.

TABLE 2 Summary statistics describing the length of juvenile Atlantic salmon, measured in the Burrishoole catchment, Co. Mayo, Ireland.

| Age class | Count | Mean | S.D. | Min | 25% | 50% | 75% | Max |
|-----------|--------|-------|------|-----|-----|-----|-----|-----|
| 0 | 22,048 | 55.4 | 7.6 | 21 | 50 | 55 | 60 | 77 |
| 1 | 9021 | 98.7 | 14.7 | 48 | 89 | 98 | 108 | 164 |
| 2 | 1284 | 120.1 | 13.9 | 80 | 110 | 120 | 130 | 166 |
| Smolt | 3366 | 138.4 | 14.7 | 101 | 128 | 137 | 147 | 214 |

Note: Age-classes were determined using Gaussian mixture model classification.

omitted from the time series. The high fidelity of the LSTM neural network when driven by the 0.5° latitude \times longitude ISIMIP phase 3a obsclim data was considered sufficient for the projection of water temperatures in the Mill Race.

From the historic to the contemporary period (1961–2019), a significant warming was found for the Mill Race. When quantified using the observed and modeled time series, the long-term increase in water temperature was ~ 0.023 and $\sim 0.017^\circ\text{C year}^{-1}$, respectively (Table 1).

3.1.2 | Length-at-age

The juvenile Atlantic salmon observations from the historical and contemporary periods (1996–2019) were a mix of age classes, as determined by a Gaussian mixture model classification (Table 2). The relationship between body length (mm) of these fish and CGDD was positive and statistically significant using 35,719 observations belonging to 23 cohorts (Kendall rank correlation coefficient; $r_\tau = 0.61, p < 0.001$). A general linear model (GLM) with a gamma family, log link, and Newey-West HAC estimator found body length to increase by approximately $0.0146 \pm 0.0002\%$ ($p < 0.001$) degree day $^{-1}$ (GLM: $\beta_1 = 1.46 \times 10^{-4} \pm 0.02 \times 10^{-4}, \beta_0 = 3.6463 \pm 0.010, R_{cs}^2 = 0.99, p < 0.001$; Figure 4).

3.2 | Future projections

3.2.1 | Water temperatures in the Mill Race

Future projections derived by coupling of the LSTM neural network and atmospheric data from the ISIMIP phase 3b climate forcing ensemble revealed warming of water temperatures in the Mill Race across the 80-year period (2020–2100) under two of the three SSP-RCP-scenarios (Figure 5). There was no significant linear long-term trend in water temperature for SSP1-RCP 2.6 ($p > 0.05$), whereas SSP3-RCP 7.0 increased by $\sim 0.02^\circ\text{C year}^{-1}$ ($p > 0.01$) and SSP5-RCP 8.5 increased by $\sim 0.03^\circ\text{C year}^{-1}$ ($p > 0.01$) (OLS: $R_{adj}^2 = 0.89$).

3.2.2 | Life-history response

When the length-at-age model is driven by the LSTM water temperature projections to simulate (1) length-at-smoltification decision; (2) length-at-smoltification as 1-year-old smolts; and (3) length-at-

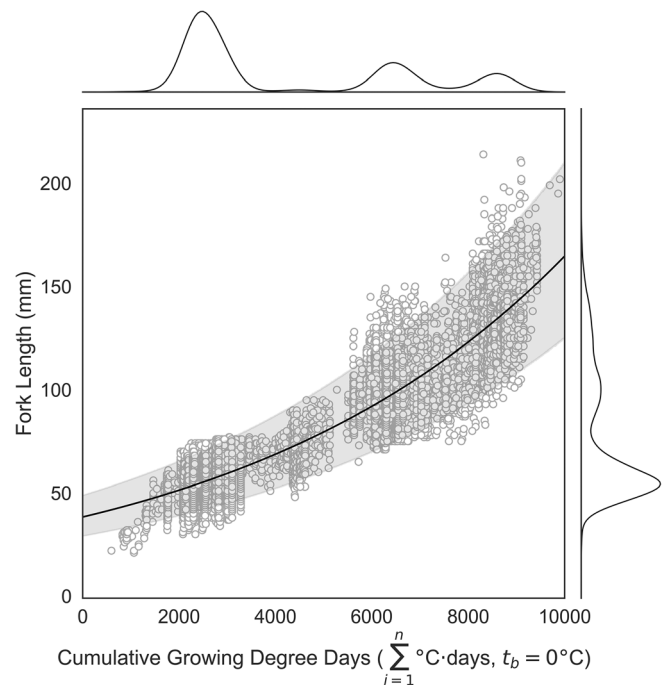


FIGURE 4 Generalized linear model of body length (mm) as a function of cumulative growing degree days (CGDD, $^\circ\text{C day}$) for the 23 observed cohorts of juvenile Atlantic salmon in the Burrishoole watershed. The solid line represents the mean length, and the gray bands represent the 95% prediction interval. The outer lines represent the sample density.

smoltification as 2-year-old smolts, the response to temperature change, in terms of growth gain, differs between the three key moments of freshwater residency (Figure 6; Table 3).

The different response to temperature changes between the key life-history events results in diverging trends in the proportion of Atlantic salmon that chose to smolt as 1-year-olds between SSP1-RCP2.6 ($\beta = -0.0002 \text{ cohort}^{-1}, p < 0.01$), SSP3-RCP7.0 ($\beta = 0.0011 \text{ cohort}^{-1}, p < 0.01$) and SSP5-RCP8.5 ($\beta = 0.0017 \text{ cohort}^{-1}, p < 0.01$), when quantified using OLS regression ($R^2 = 0.830, F(5, 228) = 222.4, p < 0.01$; Figure 7).

Using OLS regression ($R^2 = 0.825, F(5, 228) = 220.1, p < 0.01$) to estimate the effects of changing smolt age proportion on population average age-at-smoltification (Figure 8), barring the effect of mortality, age-at-smoltification had an initial decrease before tending toward current age-at-smoltification under SSP1-RCP2.6 ($\beta = -0.0002, p < 0.01$), but decreased under SSP3-RCP7.0 ($\beta = -0.0011, p < 0.01$) and SSP-RCP8.5 ($\beta = -0.0017, p < 0.01$).

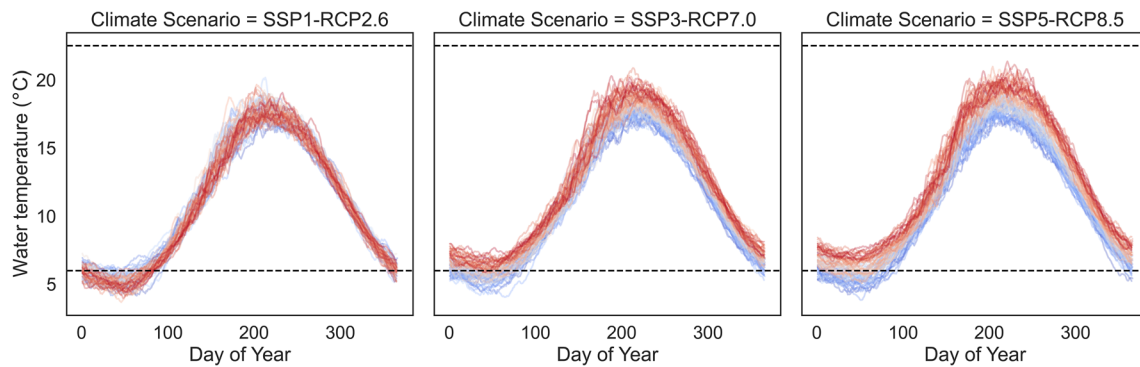


FIGURE 5 Ensemble average daily water temperature by day of year for the future projections under the three shared socioeconomic pathways and representative concentration pathways (SSP1-RCP2.6 left, SSP3-RCP7.0 middle, and SSP5-RCP8.5 right). Each line represents the day of year average temperature for the climate forcing ensemble with colors transitioning from blue to red toward the end of the century (starting with 2020 and ending with 2100). The lower dashed line represents the lower growth threshold temperature of 7°C, and the upper dashed line represents the upper growth threshold temperature for 23°C (Elliott & Hurley, 1997).

4 | DISCUSSION

This study provides a data-efficient approach to simulating length-at-age in ectotherms under historical, contemporary, and future climates using the ISIMIP framework. The potential of the approach is demonstrated by elucidating life-history responses of the migratory, cold-water-evolved Atlantic salmon under historical, contemporary, and three future climate warming scenarios.

As has been previously reported, growth in ectotherms follows thermal clines, with higher temperatures causing faster growth and earlier maturation (Angilletta et al., 2004). For the Atlantic salmon, this is ascribed to the combination of temperature and photoperiod (Metcalf & Thorpe, 1990; Power, 1981, 1986). This study shows that water temperatures in the geographic area encompassing the Burrishoole catchment will shift closer to the optimal growth temperature of ~16°C for Atlantic salmon parr proposed by Elliott and Hurley (1997) under SSP3-RCP7.0 and SSP5-RCP8.5, whereas SSP1-RCP2.6 appears to remain close to contemporary conditions. Moreover, with respect to the two most severe warming scenarios, it shows a lengthening of the growth season by temperature (i.e., the period of time within which temperatures of 7 to 23°C are experienced) is expected, which effectively translates into an increase in growth potential for juvenile Atlantic salmon in the Burrishoole River system over the century.

An increase in growth potential will, if realized, cause increased growth rates, which is here shown as an increase in the length-at-age for juvenile Atlantic salmon in the Burrishoole. This finding is in line with Hedger et al. (2013), Piou and Prévost (2012), Sundt-Hansen et al. (2018), all showing faster growth during freshwater residency. For Atlantic salmon, growth rate will cause changes in life-history traits age- and size-at-smoltification, which will have carry-over effects on marine survival, age- and size-at-reproduction, and reproductive investment (Gregory et al., 2019; Jonsson & Jonsson, 2007; Mobley et al., 2020).

In Atlantic salmon, the decision to smoltify is made in late summer the year prior to spring migration and is based on energetic status and

growth rate at that time and the likelihood of reaching a threshold length at the time of migration (Metcalf, 1998; Thorpe et al., 1998). Our results show that the increase in growth rate caused by temperature will lead to an increase in the proportion of juveniles that satisfy the conditions for smoltification as 1-year-olds and a reduction in the proportion of juveniles that require 3 years to satisfy these conditions. In accordance with the findings of Russell et al. (2012), Piou & Prévost, 2012, Hedger et al., 2013, and Sundt-Hansen et al., 2018, we find a decrease in the age-at-smoltification measured at the population level in response to the temperature increase under SSP3-RCP7.0 and SSP5-RCP8.5, but for SSP1-RCP 2.6 the reversal of the GHG concentrations causes the initial decrease in age-at-smoltification, which is gradually reversed over the century.

Sundt-Hansen et al. (2018) associated this reduction in freshwater residency (implicit from a decrease in age-at-smoltification) with a shortening of the period subject to density-dependent mortality, which would result in an increased smolt abundance. However, ambient temperatures regulate metabolism, and thus resource requirements, and may potentially strengthen density-dependent mortality even if the period in which the density-dependent mortality occurs is shortened. Further, a decrease in age-at-smoltification is likely to entail a reduction in size-at-smoltification due to the migration window usually occurring once every year. Accordingly, when increasing temperatures push a growth rate previously resulting in a 2-year-smoltification trajectory into a 1-year-smoltification trajectory, it results in the loss of an entire year of freshwater growth. Consequently, the faster growth trajectories with a marginal improvement in growth will likely not compensate for this loss of freshwater growth. There will, however, be an increase in length-at-smoltification within smolt age groups as the total growth potential between migration windows increases.

The consequence of a reduction in age- and size-at-smoltification on population vital rates is unclear. Gregory et al. (2019) showed that marine survival, measured from time of smoltification to return as one sea-winter spawner, is positively correlated with body size at the time of smoltification, whereas Jonsson and Jonsson (2007) and Mobley

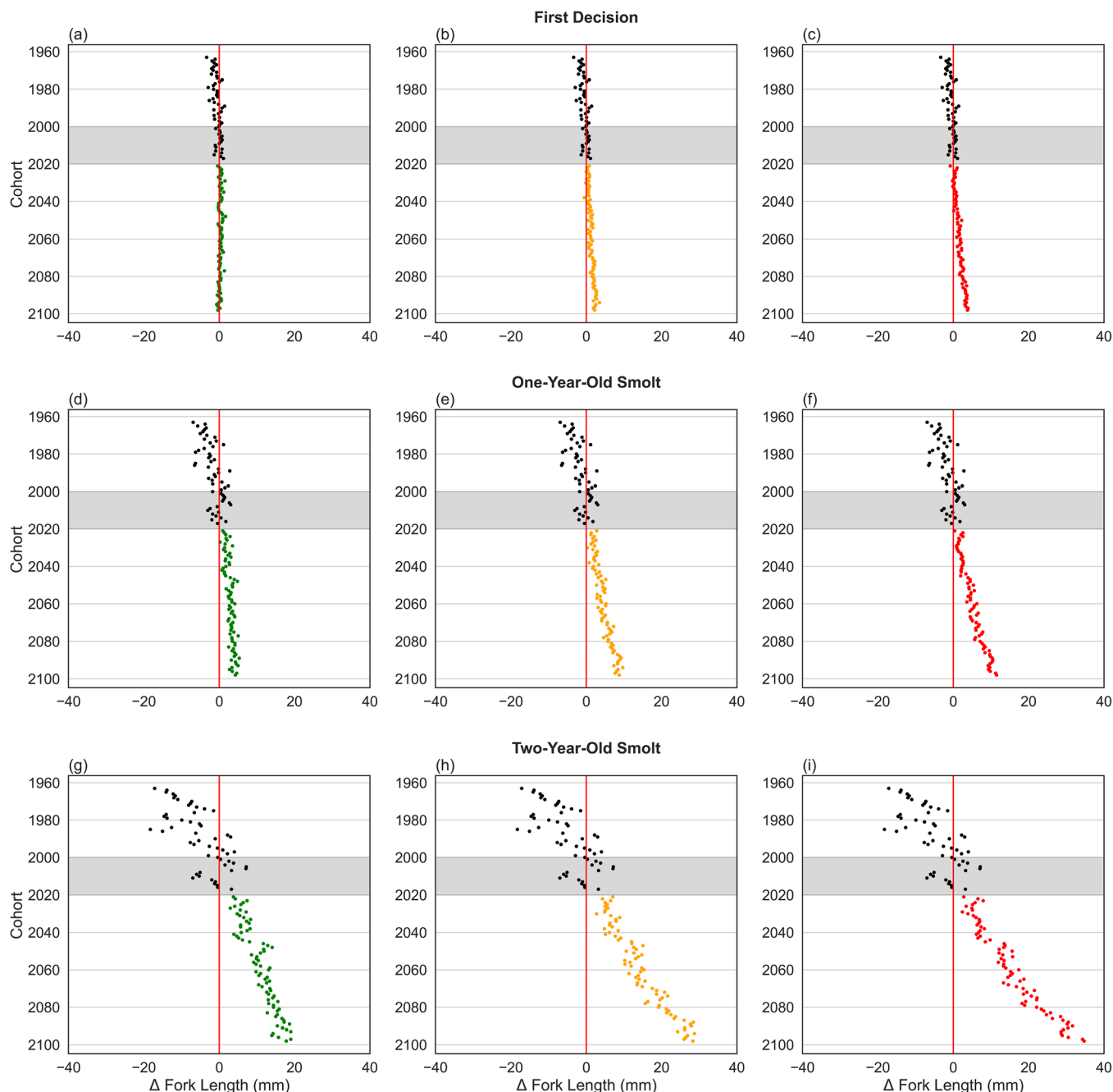


FIGURE 6 Projected change between 1960 and 2100 in length-at-smoltification decision (a, b, and c), length-at-smoltification as 1-year-olds (d, e, and f), and length-at-smoltification as 2-year-olds (g, h, and i) under the three shared socioeconomic pathways and representative concentration pathways: SSP1-RCP2.6 (green), SSP3-RCP7.0 (orange), and SSP5-RCP8.5 (red) for juvenile Atlantic salmon in the Burrishoole. The gray-shaded area represents the historical reference (2000 to 2020), and the red vertical line represents the historical average.

et al. (2020) showed that females migrating at a younger age had a higher propensity to return as multi sea-winter aged spawners (MSW). Jonsson and Jonsson (2007) attributed this increased propensity to return as MSW to an increased growth rate over the first sea-winter, but they also pointed out that the relationship between early marine growth and sea age is likely to be population-specific and might even vary in sign across regions. How this will play out when growth rates increase because of climate change is difficult to predict, as these

younger migrants are likely to reach greater body size and therefore lower relative growth rates. If the consequences of temperature increases follow the temperature-size rule and the intraspecific formulation of Bergmann's rule (Angilletta et al., 2004; Ashton, 2004; Blackburn et al., 1999), then a decrease in body size of adult spawners in the Burrishoole is to be expected. Smaller body size in Atlantic salmon, and fish in general, typically corresponds to a disproportional decrease in reproductive output (Barneche et al., 2018). Further, the

TABLE 3 Ordinary least squares regression of change in length (mm) scaled to the 2000–2020 historical reference length at (1) length-at-smoltification decision, (2) length-at-smoltification (1-year-olds), and (3) length-at-smoltification (2-year-olds) under SSP1-RCP2.6, SSP3-RCP7.0, and SSP5-RCP8.5 for juvenile Atlantic salmon in the Burrishoole catchment, Co. Mayo, Ireland.

| | Length at decision | Length at smoltification (1-year-old) | Length at smoltification (2-year-old) |
|----------------------|--------------------|---------------------------------------|---------------------------------------|
| SSP1-RCP2.6 | 65.21*** (4.47) | 7.75*** (8.85) | −211.12*** (21.76) |
| SSP3-RCP7.0 | −72.66*** (6.32) | −125.21*** (12.52) | −283.04*** (30.77) |
| SSP5-RCP8.5 | −107.62*** (6.32) | −184.17*** (12.52) | −411.82*** (30.77) |
| Cohort * SSP1-RCP2.6 | −0.01*** (0.00) | 0.03*** (0.00) | 0.17*** (0.01) |
| Cohort * SSP3-RCP7.0 | 0.04*** (0.00) | 0.06*** (0.01) | 0.14*** (0.01) |
| Cohort * SSP5-RCP8.5 | 0.05*** (0.00) | 0.09*** (0.01) | 0.20*** (0.01) |
| R^2 | 0.82 | 0.88 | 0.92 |
| R^2 adj. | 0.82 | 0.88 | 0.92 |
| N (DF) | 234 (228) | 234 (228) | 234 (228) |

Note: Standard errors in parentheses. * $p < 0.1$, ** $p < 0.05$, *** $p < 0.01$.

Abbreviation: SSP-RCPs, shared socioeconomic pathways and representative concentration pathways.

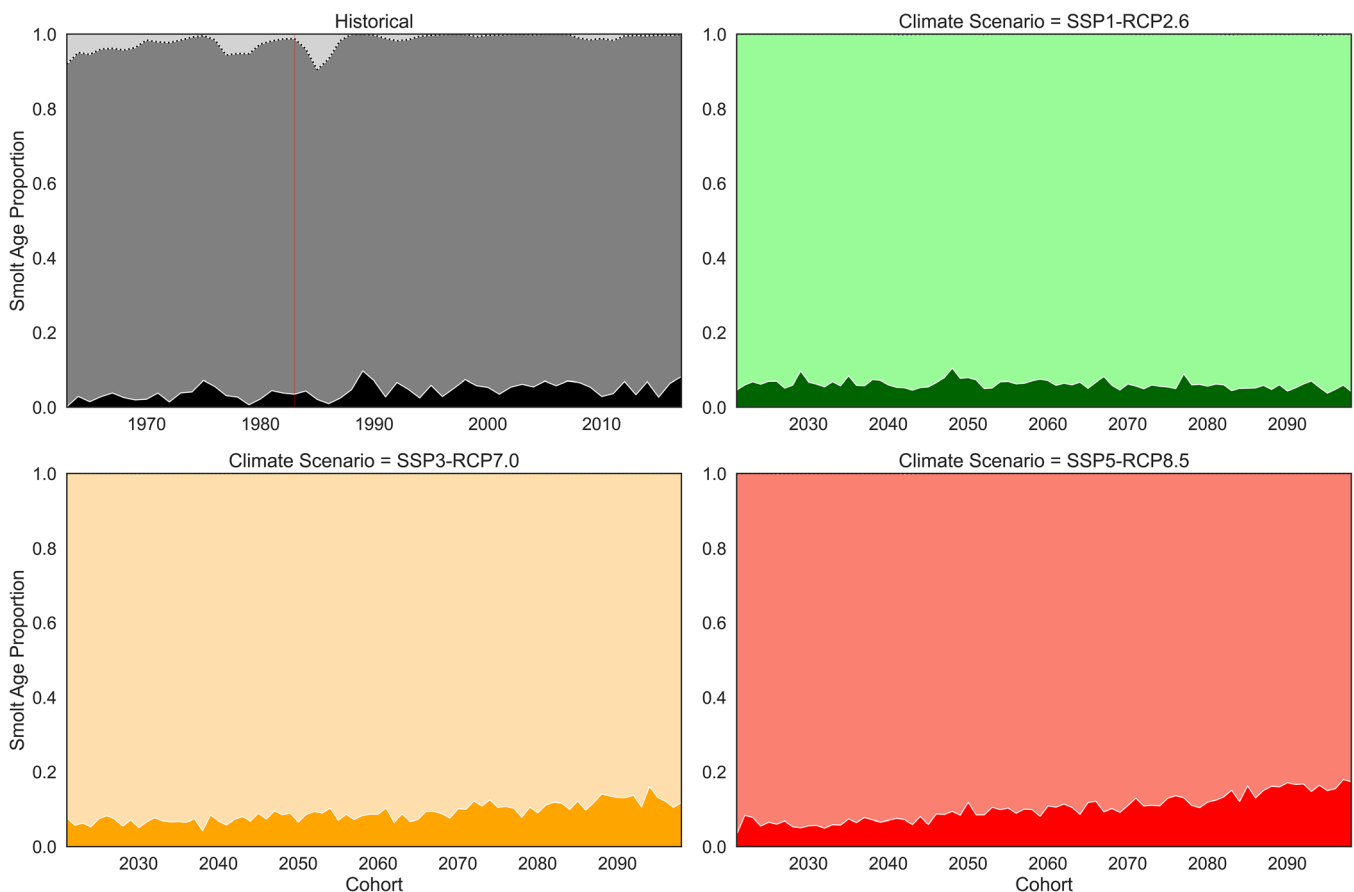


FIGURE 7 Model prediction of the proportion of juvenile Atlantic salmon choosing to smolt as 1-year-olds (full saturation, black = historical, green = SSP1-RCP2.6, orange = SSP3-RCP7.0, and red = SSP5-RCP8.5), 2-year-olds (medium saturation, black = historical, green = SSP1-RCP2.6, orange = SSP3-RCP7.0, and red = SSP5-RCP8.5), and 3-year-olds (low saturation, black = historical, green = SSP1-RCP2.6, orange = SSP3-RCP7.0, and red = SSP5-RCP8.5). The red line is the point of reaction norm calibration to Piggins and Mills (1985).

disappearance of 3-year-old smolts is also a direct loss of life-history diversity, which could then be associated with reductions in population stability (Greene et al., 2010; Schindler et al., 2010).

On the basis of the differing impacts projected under SSP1-RCP2.6, SSP3-RCP7.0, and SSP5-RCP8.5, it is evident that anthropogenic influence on climate will have major implications for the future

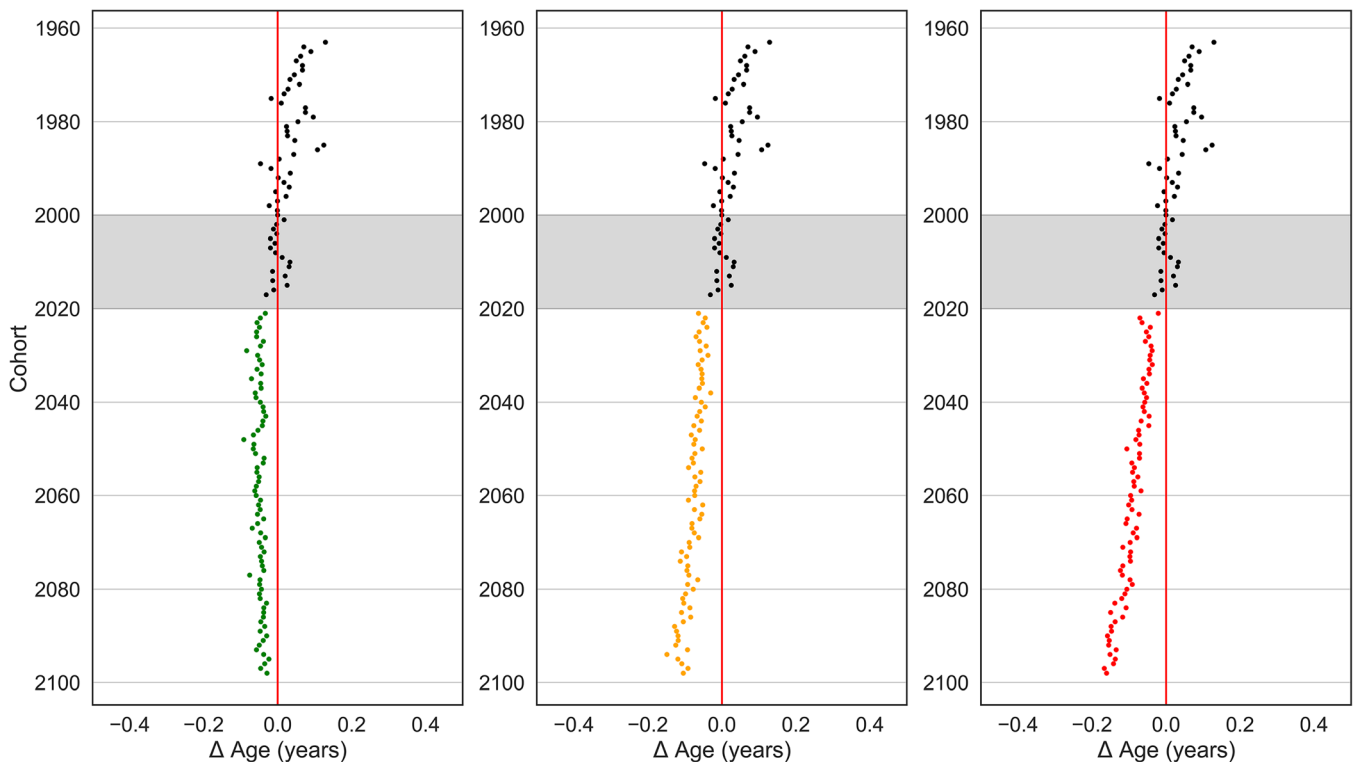


FIGURE 8 Projected change in age-at-smoltification under the three shared socioeconomic pathways and representative concentration pathways: (a) SSP1-RCP2.6 (green), (b) SSP3-RCP7.0 (orange), and (c) SSP5-RCP8.5 (red) for juvenile Atlantic salmon in the Burrishoole. The gray-shaded area represents the historical reference (2000 to 2020), and the red vertical line represents the historical average.

of Atlantic salmon in the Burrishoole. It is possible given the most optimistic response, as described in SSP1-RCP2.6, that climate change impacts on Atlantic salmon may be reversed by the end of the century. In stark contrast, gradually increasing impacts to the Atlantic salmon in the Burrishoole are projected under the SSP3-RCP7.0 and SSP5-RCP8.5 scenarios, potentially leading to reduced marine survival, reduced size- and age-at-reproduction, and reduced reproductive output. However, the prospects under SSP3-RCP7.0 are better than those for SSP5-RCP8.5 as the population is given a better opportunity to adapt to climate change (see Reed, Schindler, Hague, et al., 2011).

In this study, we demonstrated the ability of an LSTM neural network to accurately estimate water temperature from the atmospheric data available from ISIMIP phase 3a. The high accuracy of the neural network on validation data indicates that it is useful for hindcasting and forecasting water temperature in near, mid, and potentially distant time. Therefore, the method is a promising approach to studying effects on climate change on juvenile Atlantic salmon when data availability for systems is poor. However, the LSTM neural network does seem to struggle with extreme temperatures. This could be due to the lack of discharge data, although the issue appears to be common for machine learning models and may be a limitation of the approach (see Feigl et al., 2021). Nevertheless, in line with the findings of Feigl et al. (2021), we found that recurrent neural networks performed better than other machine learning and traditional regression approaches when long-term dependencies are relevant (i.e., temperature-

buffering of an upstream lake relative to the temperature monitoring station; see supplementary material S1a).

The study shows that the CGDD, when calculated from water temperature, is an excellent general predictor of length-at-age in juvenile Atlantic salmon. However, several discontinuities in the relationship occur between size-at-age and CGDD at points in time that correspond to life-history stage transitions, notably alevin (i.e., endogenous energy source via the yolk sac) to fry, and potentially parr to smolt (Neuheimer & Taggart, 2007). These discontinuities may entail the need for a more complex model, or combination of several models, when quantifying the relationship between CGDD and length-at-age over the span of several life stages. Nevertheless, in this case, the use of a GLM with a gamma distribution and log-link successfully captured the growth trajectory of the juvenile Atlantic salmon in the Burrishoole catchment. However, we are aware that the underlying mechanisms for life-stage transition are dependent on genetics and growth, which again depends on temperature, photoperiod, productivity, and fish density, and that these interactions may become difficult to predict in future climates.

The first observed discontinuity in the length-at-age CGDD relationship occurred during the alevin-fry life-stage transition (i.e., fish < 38 mm). The transition between alevin and fry life-stage requires energy allocation into development of physical structures required for the ingestion and digestion of exogenous food (Skoglund et al., 2011). The transition is also characterized by a shift in behavior from passively hiding in the interstitial spaces of riverbed substrates to actively

foraging (Einum & Fleming, 2004). This shift from endogenous to exogenous nutrition also involves the start of intraspecific competition and territory establishment, after a period of higher densities sustained by the use of resources acquired by parental fish in the marine environment. Therefore, it is reasonable to assume that the relationship between length-at-age and CGDD may deviate from that found for other life stages. A potential second discontinuity in the relationship between length-at-age and CGDD occurs during the parr-smolt life-stage transition (i.e., apparent from fish ≥ 90 mm) due to the smoltification process. According to Kadri et al. (1996), Kristinsson et al. (1985), Metcalfe (1998), Saunders et al. (1994), and Skilbrei (1988), growth of juvenile Atlantic salmon accelerates when the life-history decision has been made.

The length-at-age CGDD relationship relies on the fact that growth is near-linear in the mid-range of temperatures (Neuheimer & Taggart, 2007). However, like other statistical methods, it does not have any track record under the extreme changes in water temperature that we may experience in the future. This study assumes that the growth response to temperature is close to a bell-shaped curve, and although our projected water temperatures do not exceed the maximum growth temperature, it may still be a shortcoming of the model. Nevertheless, it is possible that the current relationship between length-at-age and CGDD breaks down given larger shifts than observed over the validation period.

This study is limited by our desire for a data-efficient, geographically transferrable, approach using only abiotic and biotic variables available for a large proportion of Atlantic salmon populations across the native range. As datasets become available for modeling other aspects of climate change impacts on juvenile Atlantic salmon, these may be added to this workflow. We are aware that this limits the ability to accurately capture important underlying processes (e.g., evolutionary responses), which determine the overall response of juvenile Atlantic salmon in a climate change context. Although this paper focuses on the plastic response of juvenile Atlantic salmon to warming temperatures, potential evolutionary responses may add further complexity. For example, Debes et al. (2020) showed that there is a heritable genetic component to growth potential that contributes to determining the smoltification reaction norm across different temperatures and productivity regimes (feeding rates). Evolution and plasticity may, therefore, act either in the same direction or in opposite directions, regarding age-at-smoltification depending on whether higher or lower growth potential is selected at higher temperatures. Further work is needed to evaluate these alternatives.

One other aspect that is worth considering is the probability of an individual smolting in the following spring. It has been proposed that this decision is made in late July (Metcalfe, 1998; Metcalfe & Thorpe, 1992) and depends on an individual's phenotypic size and an assessment of its energetic status. Furthermore, Debes et al. (2020) suggest that there is also a genetic component to this decision. Those individuals that postpone smoltification, as an adaptive response to the expected local winter conditions, in the following spring are observed to downregulate metabolism, suspend feeding, and adopt an

anorexic state despite adequate food availability (Metcalfe & Thorpe, 1992). Given that there will likely be changes to winter thermal regimes (i.e., warmer winters) in the future, it might be assumed that this contemporary adaptive response to overwintering could change. Although warmer winters might simplistically be presumed to be less harsh, it is more likely that they will be more severe due to heightened energetic demands and insufficient food to sustain higher metabolic demands. This has been shown in several important studies (Bradshaw & Holzapfel, 2006; Humphries et al., 2002; McGinnity et al., 2009). Warmer winter temperatures are therefore likely to select against the torpor strategy in the future as an effective strategy for overwinter survival and thus favor faster-growing individuals and result in an increased pace of life for the population overall.

However, these limitations do not imply that we cannot identify changes to existing large-scale trends, such as the ones driven by temperature. An example of this would be the underestimated length distribution of 1-year-old smolt, as we are unable to quantify growth for fish in the 1-year-smolt trajectory after the smoltification decision. Nevertheless, the growth response only causes a positive shift in the length distribution, and the mechanism remains the same, implying that it captures the large-scale trend. Moreover, the model may not be robust due to the inherent uncertainty tied to extrapolation, and the model chain has only been applied to one study system; the generalizability of the model workflow should be applied to several systems for validation. An improvement to the model workflow may be obtained by re-estimation of Equation (2) from Metcalfe (1998), which is derived from hatchery-reared fish, and does, most likely, overestimate the smoltification probability found in the Burrishoole River system due to differences in growth rates and resource limitations.

In conclusion, this study provides a data-efficient model workflow applicable to ectotherms, in particular aquatic ectotherms, for investigation of their life-history response to historical, contemporary, and future climates. The potential of the model, although simplistic relative to the underlying mechanisms, is shown by its ability to reproduce findings in line with more complex and data-demanding approaches, as well as expectations founded in best available knowledge on the Atlantic salmon. Although the geographical transferability of the model remains untested, the underlying data are commonly found throughout the native range of the Atlantic salmon. This enables the transfer of the model from data-rich to data-poor systems, allowing a range-wide examination of climate impacts on Atlantic salmon. More generally, our modeling work emphasizes how increased growth potential in ectotherms as a result of global warming can filter through the life cycle in complex ways, potentially speeding up the overall pace of life.

AUTHOR CONTRIBUTIONS

Conceptualization: Adrian Rinaldo, Elvira de Eyto, Philip McGinnity, Thomas Reed. Developing methods: Adrian Rinaldo, Elvira de Eyto, Philip McGinnity, Karl Øystein Gjelland. Data analysis: Adrian Rinaldo. Preparation of figures and tables: Adrian Rinaldo. Conducting the research, data interpretation, writing: Adrian Rinaldo, Elvira de Eyto, Philip McGinnity, Thomas Reed, Karl Øystein Gjelland.

ACKNOWLEDGMENTS

This project has received funding from the European Union's Horizon 2020 research and innovation programme under the Marie Skłodowska-Curie grant agreement no. 956623. MSCA-ITN-ETN-European Training Network, inventWater (<https://inventwater.eu/>). P. M. was supported in part by grants from Science Foundation Ireland (15/IA/3028 and 16/BBSRC/3316) and by grant-in-aid (RESPI/BIO/21/01) from the Marine Institute (Ireland) as part of the Marine Research Programme by the Irish Government. Further, we acknowledge the Inter-Sectoral Impact Model Intercomparison Project (ISI-MIP) for their role as provider and coordinator of climate data. The in-situ data collection for this work was carried out by the many staff of the Marine Institute (formerly the Salmon Research Agency and the Salmon Research Trust of Ireland). Their contribution is gratefully acknowledged. Eva Bonsak Thorstad, Joshka Kaufmann, and Ian Jones provided helpful comments throughout this work. Open access funding provided by IReL.

DATA AVAILABILITY STATEMENT

The code, models, and projections used for this article are available at <https://github.com/AdrianRinaldo/Size-at-Age-Juvenile-Atlantic-Salmon>. The climatological (atmospheric) data are available at <https://data.isimip.org/>. Fish size data (lengths) from the Burrishoole catchment are openly accessible from <https://data.marine.ie/geonetwork/srv/eng/catalog.search#/metadata/ie.marine.data:data.5125>.

ORCID

Adrian Rinaldo  <https://orcid.org/0009-0007-4832-3684>

REFERENCES

- Abadi, M., Barham, P., Chen, J., Chen, Z., Davis, A., Dean, J., Devin, M., Ghemawat, S., Irving, G., Isard, M., Kudlur, M., Levenberg, J., Monga, R., Moore, S., Murray, D. G., Steiner, B., Tucker, P., Vasudevan, V., Warden, P., ... Zheng, X. (2016). TensorFlow: A system for large-scale machine learning. *Proceedings of the 12th USENIX Symposium on Operating Systems Design and Implementation, OSDI 2016*.
- Angilletta, M. J., Steury, T. D., & Sears, M. W. (2004). Temperature, growth rate, and body size in ectotherms: Fitting pieces of a life-history puzzle. *Integrative and Comparative Biology*, 44(6), 498–509. <https://doi.org/10.1093/icb/44.6.498>
- Ashton, K. G. (2004). Sensitivity of intraspecific latitudinal clines of body size for tetrapods to sampling, latitude and body size. *Integrative and Comparative Biology*, 44(6), 403–412. <https://doi.org/10.1093/icb/44.6.403>
- Atkinson, D. (1994). Temperature and organism size—A biological law for ectotherms? In M. Begon, & A. H. Fitter (Eds.), *Advances in ecological research* (Vol. 25, pp. 1–58). [https://doi.org/10.1016/S0065-2504\(08\)60212-3](https://doi.org/10.1016/S0065-2504(08)60212-3)
- Barneche, D. R., Ross Robertson, D., White, C. R., & Marshall, D. J. (2018). Fish reproductive-energy output increases disproportionately with body size. *Science*, 360, 642–645. <https://doi.org/10.1126/science.aao6868>
- Bennett, J. M., Sunday, J., Calosi, P., Villalobos, F., Martínez, B., Molina-Venegas, R., Araújo, M. B., Algar, A. C., Clusella-Trullas, S., Hawkins, B. A., Keith, S. A., Kühn, I., Rahbek, C., Rodríguez, L., Singer, A., Morales-Castilla, I., & Olalla-Tárraga, M. Á. (2021). The evolution of critical thermal limits of life on earth. *Nature Communications*, 12(1), 1198. <https://doi.org/10.1038/s41467-021-21263-8>
- Blackburn, T. M., Gaston, K. J., & Loder, N. (1999). Geographic gradients in body size: A clarification of Bergmann's rule. *Diversity and Distributions*, 5(4), 165–174. <https://doi.org/10.1046/j.1472-4642.1999.00046.x>
- Bradshaw, W. E., & Holzapfel, C. M. (2006). Evolutionary response to rapid climate change. *Science*, 312(5779), 1477–1478. <https://doi.org/10.1126/science.1127000>
- Chezik, K. A., Lester, N. P., & Venturelli, P. A. (2014). Fish growth and degree-days I: Selecting a base temperature for a within-population study. *Canadian Journal of Fisheries and Aquatic Sciences*, 71(1), 47–55. <https://doi.org/10.1139/cjfas-2013-0295>
- Chollet, F. (2013). Keras. *Journal of Chemical Information and Modeling*, 53(9). <https://keras.io>
- Crozier, L. G., Hendry, A. P., Lawson, P. W., Quinn, T. P., Mantua, N. J., Battin, J., Shaw, R. G., & Huey, R. B. (2008). Potential responses to climate change in organisms with complex life histories: Evolution and plasticity in Pacific salmon. *Evolutionary Applications*, 1(2), 252–270. <https://doi.org/10.1111/j.1752-4571.2008.00033.x>
- de Eyto, E., Kelly, S., Rogan, G., French, A., Cooney, J., Murphy, M., Nixon, P., Hughes, P., Sweeney, D., & McGinnity, P. (2022). Decadal trends in the migration phenology of diadromous fishes native to the Burrishoole catchment, Ireland. *Frontiers in Ecology and Evolution*, 640, 19. <https://doi.org/10.3389/fevo.2022.915854>
- Debes, P. V., Piavchenko, N., Erkinaro, J., & Primmer, C. R. (2020). Genetic growth potential, rather than phenotypic size, predicts migration phenotype in Atlantic salmon. *Proceedings of the Royal Society B: Biological Sciences*, 287(1931), 20200867. <https://doi.org/10.1098/rspb.2020.0867>
- Einum, S., & Fleming, I. A. (2004). Does within-population variation in egg size reduce intraspecific competition in Atlantic Salmon, *Salmo salar*? *Functional Ecology*, 18(1), 110–115. <https://doi.org/10.1111/j.1365-2435.2004.00824.x>
- Elliott, J. M. (1991). Tolerance and resistance to thermal stress in juvenile Atlantic salmon, *Salmo salar*. *Freshwater Biology*, 25(1), 61–70. <https://doi.org/10.1111/j.1365-2427.1991.tb00473.x>
- Elliott, J. M., & Elliott, J. A. (2010). Temperature requirements of Atlantic salmon *Salmo salar*, brown trout *Salmo trutta* and Arctic charr *Salvelinus alpinus*: Predicting the effects of climate change. *Journal of Fish Biology*, 77(8), 1793–1817. <https://doi.org/10.1111/j.1095-8649.2010.02762.x>
- Elliott, J. M., & Hurley, M. A. (1997). A functional model for maximum growth of Atlantic Salmon parr, *Salmo salar*, from two populations in Northwest England. *Functional Ecology*, 11(5), 592–603. <https://doi.org/10.1046/j.1365-2435.1997.00130.x>
- Feigl, M., Lebedzinski, K., Herrnegger, M., & Schulz, K. (2021). Machine-learning methods for stream water temperature prediction. *Hydrology and Earth System Sciences*, 25(5), 2951–2977. <https://doi.org/10.5194/hess-25-2951-2021>
- Frieler, K., Lange, S., Piontek, F., Reyer, C. P. O., Schewe, J., Warszawski, L., Zhao, F., Chini, L., Denvil, S., Emanuel, K., Geiger, T., Halladay, K., Hurtt, G., Mengel, M., Murakami, D., Ostberg, S., Popp, A., Riva, R., Stevanovic, M., ... Yamagata, Y. (2017). Assessing the impacts of 1.5 C global warming – Simulation protocol of the inter-sectoral impact model Intercomparison project (ISIMIP2b). *Geoscientific Model Development*, 10(12), 4321–4345. <https://doi.org/10.5194/gmd-10-4321-2017>
- Greene, C. M., Hall, J. E., Guilbault, K. R., & Quinn, T. P. (2010). Improved viability of populations with diverse life-history portfolios. *Biology Letters*, 6(3), 382–386. <https://doi.org/10.1098/rsbl.2009.0780>
- Gregory, S. D., Ibbotson, A. T., Riley, W. D., Nevoux, M., Lauridsen, R. B., Russell, I. C., Britton, J. R., Gillingham, P. K., Simmons, O. M., Rivot, E., & Durif, C. (2019). Atlantic salmon return rate increases with smolt length. *ICES Journal of Marine Science*, 76(6), 1702–1712. <https://doi.org/10.1093/icesjms/fsz066>
- Hazel, J. R., & Prosser, C. L. (1974). Molecular mechanisms of temperature compensation in poikilotherms. *Physiological Reviews*, 54(3), 620–677. <https://doi.org/10.1152/physrev.1974.54.3.620>

- Hedger, R. D., Sundt-Hansen, L. E., Forseth, T., Ugedal, O., Diserud, O. H., Kvambekk, Å. S., & Finstad, A. G. (2013). Predicting climate change effects on subarctic-arctic populations of Atlantic salmon (*Salmo salar*). *Canadian Journal of Fisheries and Aquatic Sciences*, 70(2), 159–168. <https://doi.org/10.1139/cjfas-2012-0205>
- Humphries, M. M., Thomas, D. W., & Speakman, J. R. (2002). Climate-mediated energetic constraints on the distribution of hibernating mammals. *Nature*, 418(6895), 313–316. <https://doi.org/10.1038/nature00828>
- ICES. (2022). Working Group on North Atlantic Salmon (WGNAS). <https://doi.org/10.17895/ices.pub.7923>
- IPCC. (2022). IPCC, 2022: Summary for policy makers. In *Climate change 2022: Impacts, Adaptation and Vulnerability*. Intergovernmental Panel on Climate Change.
- Jensen, A. J., Johnsen, B. O., & Heggberget, T. G. (1991). Initial feeding time of Atlantic salmon, *Salmo salar*, alevins compared to river flow and water temperature in Norwegian streams. *Environmental Biology of Fishes*, 30(4), 379–385. <https://doi.org/10.1007/BF02027981>
- Jonsson, B., & Jonsson, N. (2009). A review of the likely effects of climate change on anadromous Atlantic salmon *Salmo salar* and brown trout *Salmo trutta*, with particular reference to water temperature and flow. In *Journal of Fish Biology*, 75(10), 2381–2447. <https://doi.org/10.1111/j.1095-8649.2009.02380.x>
- Jonsson, N., & Jonsson, B. (2007). Sea growth, smolt age and age at sexual maturation in Atlantic salmon. *Journal of Fish Biology*, 71(1), 245–252. <https://doi.org/10.1111/j.1095-8649.2007.01488.x>
- Kadri, S., Mitchell, D. F., Metcalfe, N. B., Huntingford, F. A., & Thorpe, J. E. (1996). Differential patterns of feeding and resource accumulation in maturing and immature Atlantic salmon, *Salmo salar*. *Aquaculture*, 142(3–4), 245–257. [https://doi.org/10.1016/0044-8486\(96\)01258-6](https://doi.org/10.1016/0044-8486(96)01258-6)
- Klemetsen, A., Amundsen, P. A., Dempson, J. B., Jonsson, B., Jonsson, N., O'Connell, M. F., & Mortensen, E. (2003). Atlantic salmon *Salmo salar* L., brown trout *Salmo trutta* L. and Arctic charr *Salvelinus alpinus* (L.): A review of aspects of their life histories. *Wiley online. Library*, 12(1), 1–59. <https://doi.org/10.1034/j.1600-0633.2003.00010.x%4010.1111%28ISSN%291600-0633.Editors-Choice-2011>
- Kristinsson, J. B., Saunders, R. L., & Wiggs, A. J. (1985). Growth dynamics during the development of bimodal length-frequency distribution in juvenile Atlantic salmon (*Salmo salar* L.). *Aquaculture*, 45(1–4), 1–20. [https://doi.org/10.1016/0044-8486\(85\)90254-6](https://doi.org/10.1016/0044-8486(85)90254-6)
- MacCrimmon, H. R., & Gots, B. L. (1979). World distribution of Atlantic Salmon, *Salmo salar*. *Journal of the Fisheries Research Board of Canada*, 36(4), 422–457. <https://doi.org/10.1139/f79-062>
- Marine Institute. (2020). *Newport research facility, annual report No. 65, 2020*. Marine Institute <https://oar.marine.ie/bitstream/handle/10793/1672/Newport%20Annual%20Report%202019.pdf?sequence=1&isAllowed=y>.
- McGinnity, P., Jennings, E., DeEyto, E., Allott, N., Samuelsson, P., Rogan, G., Whelan, K., & Cross, T. (2009). Impact of naturally spawning captive-bred Atlantic salmon on wild populations: Depressed recruitment and increased risk of climate-mediated extinction. *Proceedings of the Royal Society B: Biological Sciences*, 276(1673), 3601–3610. <https://doi.org/10.1098/rspb.2009.0799>
- McGinnity, P., Stone, C., Taggart, J. B., Cooke, D., Cotter, D., Hynes, R., McCamley, C., Cross, T., & Ferguson, A. (1997). Genetic impact of escaped farmed Atlantic salmon (*Salmo salar* L.) on native populations: Use of DNA profiling to assess freshwater performance of wild, farmed, and hybrid progeny in a natural river environment. *ICES Journal of Marine Science*, 54(6), 998–1008. [https://doi.org/10.1016/s1054-3139\(97\)80004-5](https://doi.org/10.1016/s1054-3139(97)80004-5)
- Meinshausen, M., Smith, S. J., Calvin, K., Daniel, J. S., Kainuma, M. L. T., Lamarque, J., Matsumoto, K., Montzka, S. A., Raper, S. C. B., Riahi, K., Thomson, A., Velders, G. J. M., & van Vuuren, D. P. P. (2011). The RCP greenhouse gas concentrations and their extensions from 1765 to 2300. *Climatic Change*, 109(1), 213–241. <https://doi.org/10.1007/s10584-011-0156-z>
- Metcalfe, N. B. (1998). The interaction between behavior and physiology in determining life history patterns in Atlantic salmon (*Salmo salar*). *Canadian Journal of Fisheries and Aquatic Sciences*, 55(S1), 93–103. <https://doi.org/10.1139/cjfas-55-s1-93>
- Metcalfe, N. B., & Thorpe, J. E. (1990). Determinants of geographical variation in the age of seaward-migrating Salmon, *Salmo salar*. *The Journal of Animal Ecology*, 59(1), 135. <https://doi.org/10.2307/5163>
- Metcalfe, N. B., & Thorpe, J. E. (1992). Anorexia and defended energy levels in over-wintering juvenile Salmon. *The Journal of Animal Ecology*, 61(1), 175. <https://doi.org/10.2307/5520>
- Mobley, K. B., Aykanat, T., Czorlich, Y., House, A., Kurko, J., Miettinen, A., Moustakas-Verho, J., Salgado, A., Sinclair-Waters, M., Verta, J. P., & Primmer, C. R. (2021). Maturation in Atlantic salmon (*Salmo salar*, Salmonidae): A synthesis of ecological, genetic, and molecular processes. In *Reviews in Fish Biology and Fisheries*, 31(3), 523–571. <https://doi.org/10.1007/s11160-021-09656-w>
- Mobley, K. B., Granroth-Wilding, H., Ellmén, M., Orell, P., Erkinaro, J., & Primmer, C. R. (2020). Time spent in distinct life history stages has sex-specific effects on reproductive fitness in wild Atlantic salmon. *Molecular Ecology*, 29(6), 1173–1184. <https://doi.org/10.1111/mec.15390>
- Neuheimer, A. B., & Taggart, C. T. (2007). The growing degree-day and fish size-at-age: The overlooked metric. *Canadian Journal of Fisheries and Aquatic Sciences*, 64(2), 375–385. <https://doi.org/10.1139/F07-003>
- Pedregosa, F., Varoquaux, G., Gramfort, A., Michel, V., Thirion, B., Grisel, O., Blondel, M., Prettenhofer, P., Weiss, R., Dubourg, V., Vanderplas, J., Passos, A., Cournapeau, D., Brucher, M., Perrot, M., & Duchesnay, É. (2011). Scikit-learn: Machine learning in python. *Journal of Machine Learning Research*, 12, 2825–2830.
- Piggins, D. J., & Mills, C. P. R. (1985). Comparative aspects of the biology of naturally produced and hatchery-reared Atlantic salmon smolts (*Salmo salar* L.). *Aquaculture*, 45(1–4), 321–333. [https://doi.org/10.1016/0044-8486\(85\)90278-9](https://doi.org/10.1016/0044-8486(85)90278-9)
- Piou, C., & Prévost, E. (2012). A demo-genetic individual-based model for Atlantic salmon populations: Model structure, parameterization and sensitivity. *Ecological Modelling*, 231, 37–52. <https://doi.org/10.1016/j.ecolmodel.2012.01.025>
- Power, G. (1981). Stock characteristics and catches of Atlantic Salmon (*Salmo salar*) in Quebec, and Newfoundland and Labrador in relation to environmental variables. *Canadian Journal of Fisheries and Aquatic Sciences*, 38(12), 1601–1611. <https://doi.org/10.1139/f81-210>
- Power, G. (1986). Physical influences on age at maturity of Atlantic salmon (*Salmo salar*): A synthesis of ideas and questions. In D. J. Meerburg (Ed.), *Salmonid age at maturity*. *Canadian Special Publication of Fisheries and Aquatic Sciences* (Vol. 89, pp. 97–101).
- Radchuk, V., Reed, T., Teplitsky, C., van de Pol, M., Charmantier, A., Hassall, C., Adamik, P., Adriaensen, F., Ahola, M. P., Arcese, P., Miguel Avilés, J., Balbontin, J., Berg, K. S., Borrás, A., Burthe, S., Clobert, J., Dehnhard, N., de Lope, F., Dhondt, A. A., ... Kramer-Schadt, S. (2019). Adaptive responses of animals to climate change are most likely insufficient. *Nature Communications*, 10(1), 14. <https://doi.org/10.1038/s41467-019-10924-4>
- Reed, T. E., Schindler, D. E., Hague, M. J., Patterson, D. A., Meir, E., Waples, R. S., & Hinch, S. G. (2011). Time to evolve? Potential evolutionary responses of Fraser river sockeye salmon to climate change and effects on persistence. *PLoS One*, 6(6), e20380. <https://doi.org/10.1371/journal.pone.0020380>
- Reed, T. E., Schindler, D. E., & Waples, R. S. (2011). Interacting effects of phenotypic plasticity and evolution on population persistence in a changing climate. *Conservation Biology*, 25(1), 56–63. <https://doi.org/10.1111/j.1523-1739.2010.01552.x>
- Riahi, K., van Vuuren, D. P., Kriegler, E., Edmonds, J., O'Neill, B. C., Fujimori, S., Bauer, N., Calvin, K., Dellink, R., Fricko, O., Lutz, W., Popp, A., Cuaserna, J. C., Kc, S., Leimbach, M., Jiang, L., Kram, T., Rao, S., Emmerling, J., ... Tavoni, M. (2017). The shared socioeconomic pathways and their energy, land use, and greenhouse gas emissions

- implications: An overview. *Global Environmental Change*, 42, 153–168. <https://doi.org/10.1016/j.gloenvcha.2016.05.009>
- Russell, I. C., Aprahamian, M. W., Barry, J., Davidson, I. C., Fiske, P., Ibbotson, A. T., Kennedy, R. J., MacLean, J. C., Moore, A., Otero, J., Potter, T., & Todd, C. D. (2012). The influence of the freshwater environment and the biological characteristics of Atlantic salmon smolts on their subsequent marine survival. *ICES Journal of Marine Science*, 69(9), 1563–1573. <https://doi.org/10.1093/icesjms/fsr208>
- Saunders, R. L., Duston, J., & Benfey, T. J. (1994). Environmental and biological factors affecting growth dynamics in relation to smolting of Atlantic salmon, *Salmo salar* L. *Aquaculture Research*, 25(1), 9–20. <https://doi.org/10.1111/j.1365-2109.1994.tb00662.x>
- Schindler, D. E., Hilborn, R., Chasco, B., Boatright, C. P., Quinn, T. P., Rogers, L. A., & Webster, M. S. (2010). Population diversity and the portfolio effect in an exploited species. *Nature*, 465(7298), 609–612. <https://doi.org/10.1038/nature09060>
- Seabold, S., & Perktold, J. (2010). Statsmodels: Econometric and statistical modeling with python. *SciPy*. <https://doi.org/10.25080/majora-92bf1922-011>
- Sears, M. W., & Angilletta, M. J. (2011). Introduction to the symposium: Responses of organisms to climate change: A synthetic approach to the role of thermal adaptation. *Integrative and Comparative Biology*, 51(5), 662–665. <https://doi.org/10.1093/icb/ucr113>
- Skilbrei, O. T. (1988). Growth pattern of pre-smolt Atlantic salmon (*Salmo salar* L.): The percentile increment method (PIM) as a new method to estimate length-dependent growth. *Aquaculture*, 69(1–2), 129–143. [https://doi.org/10.1016/0044-8486\(88\)90192-5](https://doi.org/10.1016/0044-8486(88)90192-5)
- Skoglund, H., Einum, S., Forseth, T., & Barlaup, B. T. (2011). Phenotypic plasticity in physiological status at emergence from nests as a response to temperature in Atlantic salmon (*Salmo salar*). *Canadian Journal of Fisheries and Aquatic Sciences*, 68(8), 1470–1479. <https://doi.org/10.1139/f2011-056>
- Sundt-Hansen, L. E., Hedger, R. D., Ugedal, O., Diserud, O. H., Finstad, A. G., Sauterleute, J. F., Tøfte, L., Alfredsen, K., & Forseth, T. (2018). Modelling climate change effects on Atlantic salmon: Implications for mitigation in regulated rivers. *Science of the Total Environment*, 631–632, 1005–1017. <https://doi.org/10.1016/j.scitotenv.2018.03.058>
- Thorpe, J. E., Mangel, M., Metcalfe, N. B., & Huntingford, F. A. (1998). Modelling the proximate basis of salmonid life-history variation, with application to Atlantic salmon, *Salmo salar* L. *Evolutionary Ecology*, 12(5), 581–599. <https://doi.org/10.1023/A:1022351814644>
- Thorstad, E. B., Bliss, D., Breau, C., Damon-Randall, K., Sundt-Hansen, L. E., Hatfield, E. M. C., Horsburgh, G., Hansen, H., Maoiléidigh, N., Sheehan, T., & Sutton, S. G. (2021). Atlantic salmon in a rapidly changing environment—Facing the challenges of reduced marine survival and climate change. *Aquatic Conservation: Marine and Freshwater Ecosystems*, 31(9), 2654–2665. <https://doi.org/10.1002/aqc.3624>
- Thorstad, E. B., Whoriskey, F., Rikardsen, A. H., & Aarestrup, K. (2011). Aquatic nomads: The life and migrations of the Atlantic Salmon. In *Atlantic Salmon ecology*. Blackwell Publishing Ltd. <https://doi.org/10.1002/9781444327755.ch1>
- Van Der Have, T. M., & De Jong, G. (1996). Adult size in ectotherms: Temperature effects on growth and differentiation. *Journal of Theoretical Biology*, 183(3), 329–340. <https://doi.org/10.1006/jtbi.1996.0224>
- van Rossum, G., & Drake, F. L. (2010). The Python Library Reference. *October*.
- Venturelli, P. A., Lester, N. P., Marshall, T. R., & Shuter, B. J. (2010). Consistent patterns of maturity and density-dependent growth among populations of walleye (*Sander vitreus*): Application of the growing degree-day metric. *Canadian Journal of Fisheries and Aquatic Sciences*, 67(7), 1057–1067. <https://doi.org/10.1139/F10-041>
- Woodward, G., Perkins, D. M., & Brown, L. E. (2010). Climate change and freshwater ecosystems: Impacts across multiple levels of organization. *Philosophical Transactions of the Royal Society B: Biological Sciences*, 365(1549), 2093–2106. <https://doi.org/10.1098/rstb.2010.0055>

SUPPORTING INFORMATION

Additional supporting information can be found online in the Supporting Information section at the end of this article.

How to cite this article: Rinaldo, A., de Eyto, E., Reed, T., Gjelland, K. Ø., & McGinnity, P. (2023). Global warming is projected to lead to increased freshwater growth potential and changes in pace of life in Atlantic salmon *Salmo salar*. *Journal of Fish Biology*, 1–15. <https://doi.org/10.1111/jfb.15603>